Integrated 3D pore architecture design of bio-based engineered catalysts and adsorbents: Preparation, chemical doping, and environmental applications

Dinh Viet Cuong [a], Jhen-Cih Wu [b], Eakalak Khan [c], Gijs Du Laing [d], Yong Sik Ok [e,*], and Chia-Hung Hou [b,f,*]

[a] *Faculty of Environmental Engineering, Hanoi University of Civil Engineering, Hanoi 100000, Vietnam*

[b] *Graduate Institute of Environmental Engineering, National Taiwan University, Taipei 10617, Taiwan*

[c] *Civil and Environmental Engineering and Construction Department, University of Nevada, Las Vegas, NV, USA*

[d] *Department of Green Chemistry and Technology, Ghent University, Ghent, Belgium*

[e] *Korea Biochar Research Center, APRU Sustainable Waste Management Program and Division of Environmental Science and Ecological Engineering, Korea University, Seoul, Republic of Korea*

[f] *Research Center for Future Earth, National Taiwan University, No. 1, Sec. 4. Roosevelt Rd., Taipei 10617, Taiwan*

*Corresponding author:

yongsikok@korea.ac.kr (Yong Sik Ok); chiahunghou@ntu.edu.tw (Chia-Hung Hou)

Supporting Information containing 14 pages, 1 table and 5 figures.

Table S1. Preparation methods and porosity characteristics of bio-based HPC/IHPC.

Precursor	Carbonization process				Pretreatment	Activation process				*SSA* (m^2 g^{-1})	*PV* (m^3 g^{-1})	R_{meso} (%)	Ref.
	Reactor type	T_c (°C)	HR_c (°C min^{-1})	t_c (h)		Activation method (Activation agent)	T_a (°C)	HR_a (°C min^{-1})	t_a (h)				
Soybean cake (O, N, and P-doped IHPC)	One-step pyrolysis	700	3	1	–	–	–	–	–	21	–	–	(Yin et al., 2019)
Bark of plane trees (S-doped-IHPC)	Pyrolysis	750	–	5	HCl washed impurities	–	–	–	–	528	0.72	–	(Xu et al., 2016)
Silk (N-doped IHPC)	–	–	–	–	–	Chemical activation ($ZnCl_2$)	900	2	1	2494	2.28	79.8	(Hou et al., 2015)
Cornhusk (O-doped IHPC)	–	–	–	–	–	Chemical activation (KOH)	800	5	1	928	0.53	26.4	(Song et al., 2015)
Sugar cane bagasse (N-doped IHPC)	–	–	–	–	–	Chemical activation ($CaCl_2$ as green activation agent)	800	5	2	946	1.39	17.7	(Liu et al., 2016)
Maple	Pyrolysis	800	5	2	–	Physical activation (Air)	350	–	7	890	0.18	–	(Chen et al., 2017)
Silkworm cocoons (N-doped IHPC)	Pyrolysis	500	–	0.5	–	Chemical activation (KOH)	900	–	2	3134	1.81	–	(Sun et al., 2017)
Chestnut (N-doped IHPC)	Pyrolysis	500	5	2	–	Chemical activation (KOH)	700	5	2	3401	2.50	25.2	(Wei et al., 2018)

Precursor	Carbonization process				Pretreatment	Activation process				*SSA* ($m^2 g^{-1}$)	*PV* ($m^3 g^{-1}$)	R_{meso} (%)	Ref.
	Reactor type	T_c (°C)	HR_c (°C min^{-1})	t_c (h)		Activation method (Activation agent)	T_a (°C)	HR_a (°C min^{-1})	t_a (h)				
Algae biomass	Pre-pyrolysis	500	2	2	HCl washed impurities	Further pyrolysis	900	2	1	416	0.38	70.0	(Tian et al., 2016)
Yeast	Pyrolysis	400	5	2	HCl washed impurities	Chemical activation (KOH)	850	5	1	3808	2.20	20.6	(Wei et al., 2019)
Natural basswood	Pyrolysis	1000	–	6	–	Physical activation (CO_2)	750	–	10	839	0.58	23.6	(Liu et al., 2018)
Soybean hulls (S-doped-IHPC)	Pyrolysis	800	3	2	HCl washed impurities	Chemical activation (KOH)	700	3	2	1232	0.54	–	(Zhu et al., 2017)
Artemia cyst shell (O-doped IHPC)	Pyrolysis	300 (+700)	1	3 (+4)	HNO_3 washed impurities	Chemical activation (KOH)	700	10	1	1758	0.76	28.9	(Zhao et al., 2015)
Silkworm cocoon (N-doped IHPC)	Pyrolysis	450	5	0.5	–	Chemical activation (KOH)	900	1	2	3386	2.20	45.5	(Sun et al., 2018)
Indicalamus leaf (IHPC)	Pyrolysis	900	5	4	HF leached metal-organic complexes template	–	–	–	–	1801	1.45	–	(Huang et al., 2017)
Tobacco stem (O, N codoped IHPC/MgO composites)	HTC	180	–	10	–	Chemical activation (KOH)	800	5	2	3156	1.90	36.3	(Zhou et al., 2020)

Precursor	Carbonization process				Pretreatment	Activation process				*SSA* ($m^2 g^{-1}$)	*PV* ($m^3 g^{-1}$)	R_{meso} (%)	Ref.
	Reactor type	T_c (°C)	HR_c (°C min^{-1})	t_c (h)		Activation method (Activation agent)	T_a (°C)	HR_a (°C min^{-1})	t_a (h)				
Porphyra (N-doped IHPC)	Pyrolysis	300 (+800)	–	1 (+2)	HNO_3 leached Ni particle template	Physical activation (Steam)	800	–	1	811	–	–	(Ouyang et al., 2019)
Soybean milk (N-doped IHPC)	–	–	–	–	HCl leached $CaCO_3$ template	Chemical activation (KOH)	700	3	2	1208	0.7	42.9	(Chen et al., 2019)
Rice straw	Pyrolysis	400	–	1	HCl leached $CaCO_3$ template	–	–	–	–	611	0.6	75.0	(Shi et al., 2020)
Green grocery (O, N-doped IHPC)	Pyrolysis	900	15	2	$ZnCl_2$ and $Mg_5(OH)_2(CO_3)_4$	–	–	–	–	1651	2.48	68.7	(Du et al., 2020)
Rice husk	Pyrolysis	500	5	1	HCl leached SiO_2 template	Physicochemical activation (KOH/CO_2)	800	5	0.5	2330	1.32	81.1	(Cuong et al., 2019)
Rice husk	Pyrolysis	900	–	1	HF leached SiO_2 template	Physical activation (N_2/steam)	850	–	0.5	861	0.35	–	(Kim et al., 2019)
Rice husk	HTC	230	–	48	NH_4HF_2 leached SiO_2 template	Higher pyrolysis	900	5	–	525	0.49	76.4	(Rybarczyk et al., 2016)
Rice husk	Pyrolysis	700	2	2	HCl leached SiO_2 template	Chemical activation (EtOH)	800	1	2	78.5	0.21	–	(Zhang et al.,

Precursor	Carbonization process: Reactor type	T_c (°C)	HR_c (°C min^{-1})	t_c (h)	Pretreatment	Activation process: Activation method (Activation agent)	T_a (°C)	HR_a (°C min^{-1})	t_a (h)	SSA (m^2 g^{-1})	PV (m^3 g^{-1})	R_{meso} (%)	Ref.
													2016)
Rice husk (MnO_2- modified IHPC)	Pyrolysis	500	–	1	NaOH leached SiO_2 template	Chemical activation (KOH)	700	–	2	1751	1.11	55.9	(Yuan et al., 2016)
Shrimp shell	Pyrolysis	400	5	2	HCl removed $CaCO_3$	Chemical activation (KOH)	850	5	2	3171	1.93	49.4	(Qin et al., 2016)
Bovine bone	Pyrolysis	400	5	2	HCl removed inorganic template	Chemical activation (KOH)	850	5	1	3232	1.98	25.8	(Dai et al., 2018)
Oyster shell + soft pitch	Pyrolysis	900	5	5	HCl leached CaO template	–	–	–	–	1258	0.58	69.6	(Gao et al., 2018)

carbonization temperature: T_c; carbonization heating rate: HR_c; carbonization time: t_c; activation temperature: T_a; activation heating rate: HR_a; activation time: t_a; specific surface area: *SSA;* total pore volume: *PV;* mesoporosity: R_{meso}

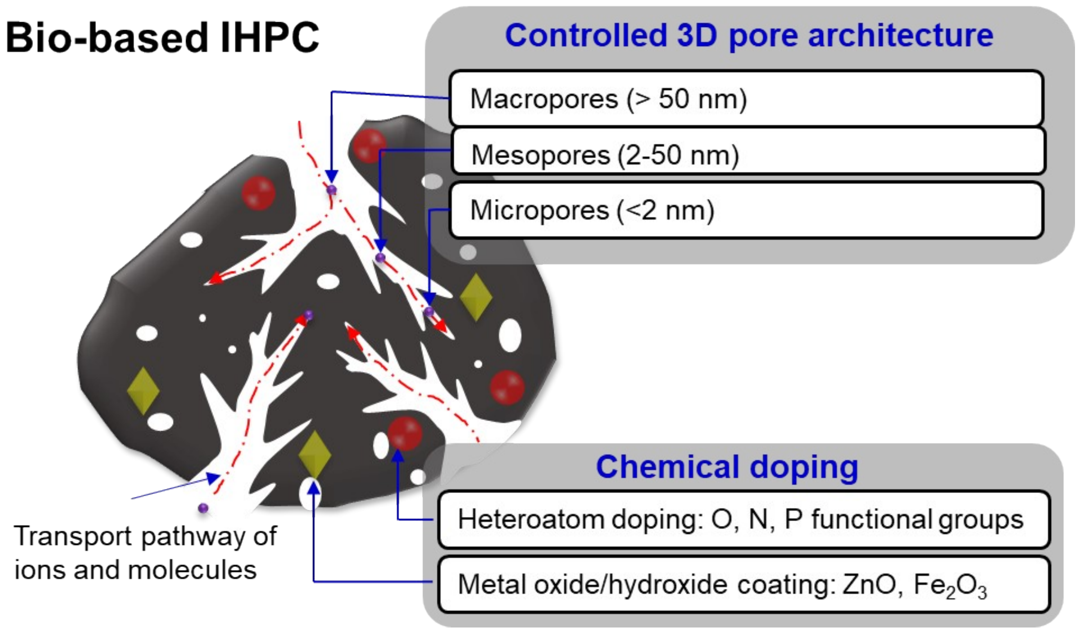

Fig. S1. Integration strategy of pore architecture design and chemical doping for bio-based IHPC. Adapted from (Cuong et al., 2021).

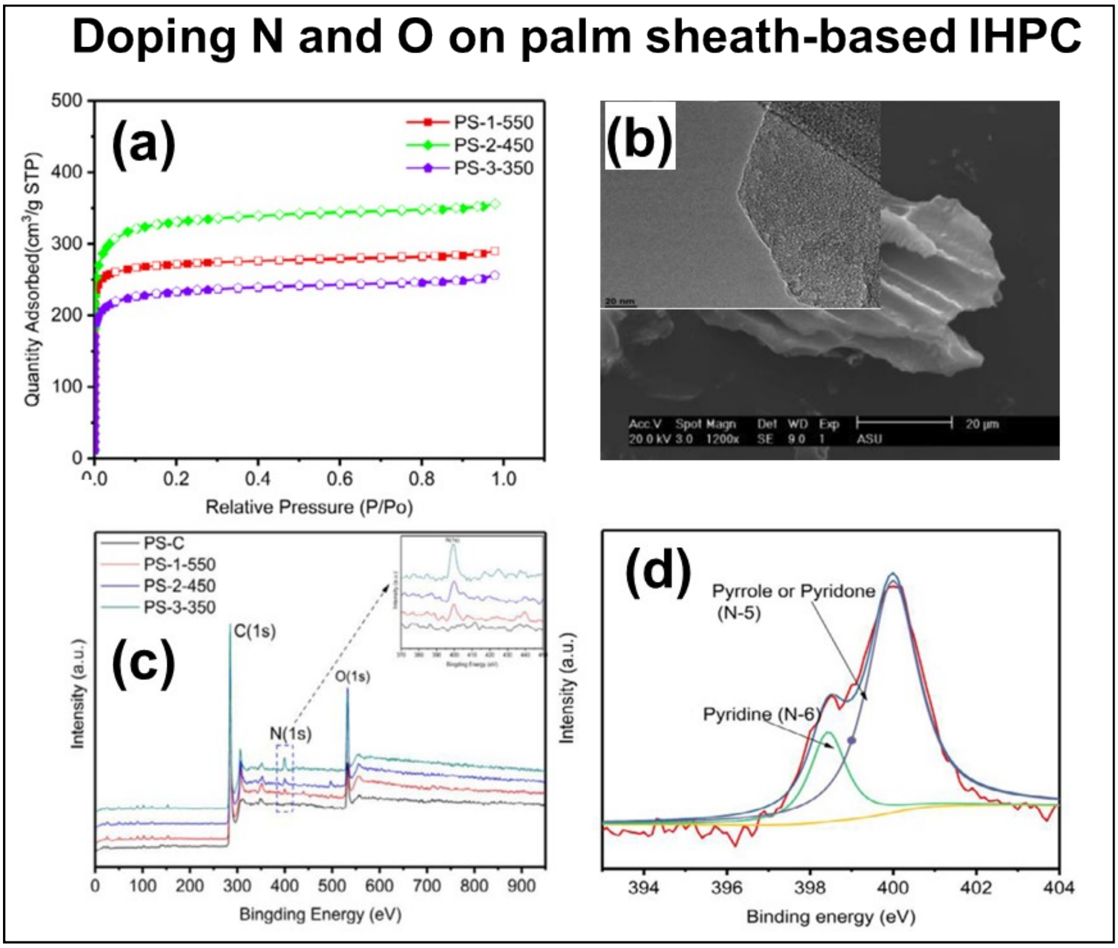

Fig. S2. (a) N_2 adsorption-desorption isotherms, (b) SEM and TEM images, (c) XPS survey spectra, (d) XPS high-resolution of N spectra of N,O-doped palm sheath-based IHPCs (Liu et al., 2020).

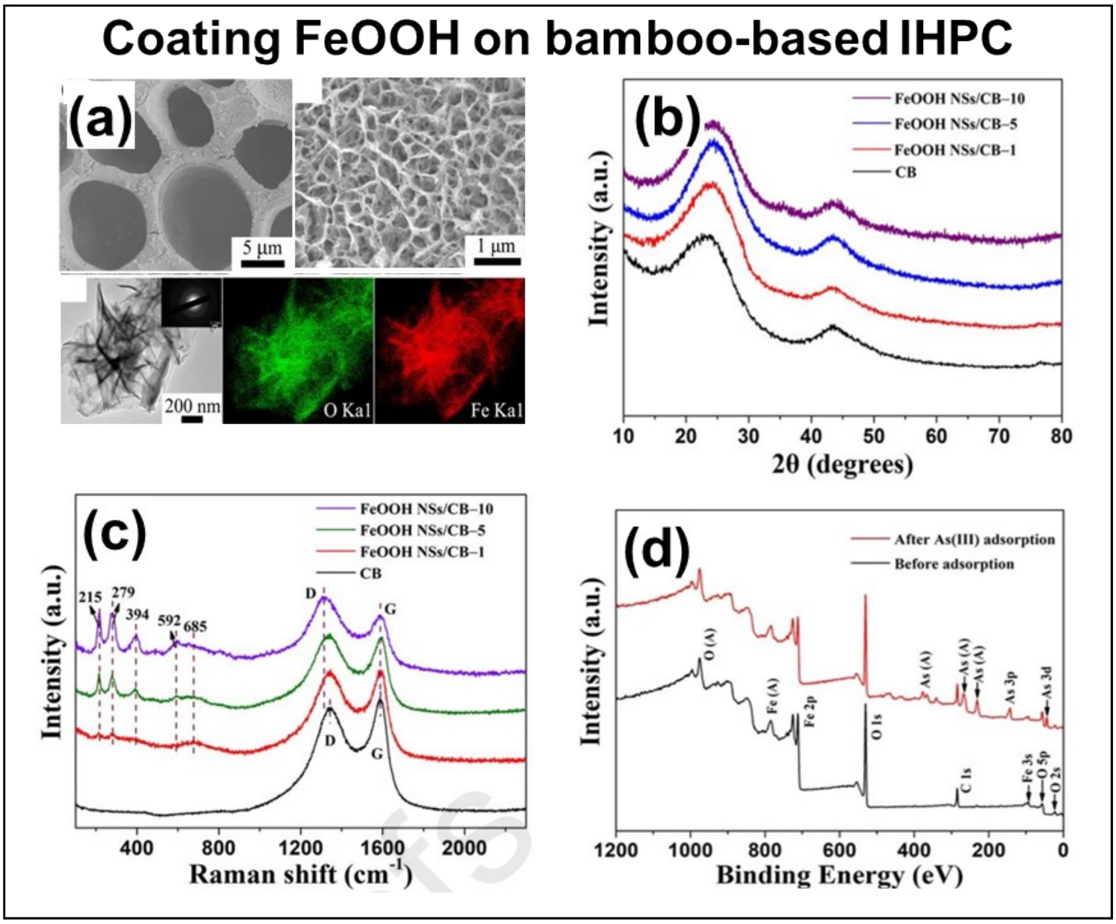

Fig. S3. (a) SEM-EDS analysis, (b) XRD spectra, (c) Raman patterns and (d) XPS analyses of FeOOH-modified bamboo-based IHPCs (Wang et al., 2020).

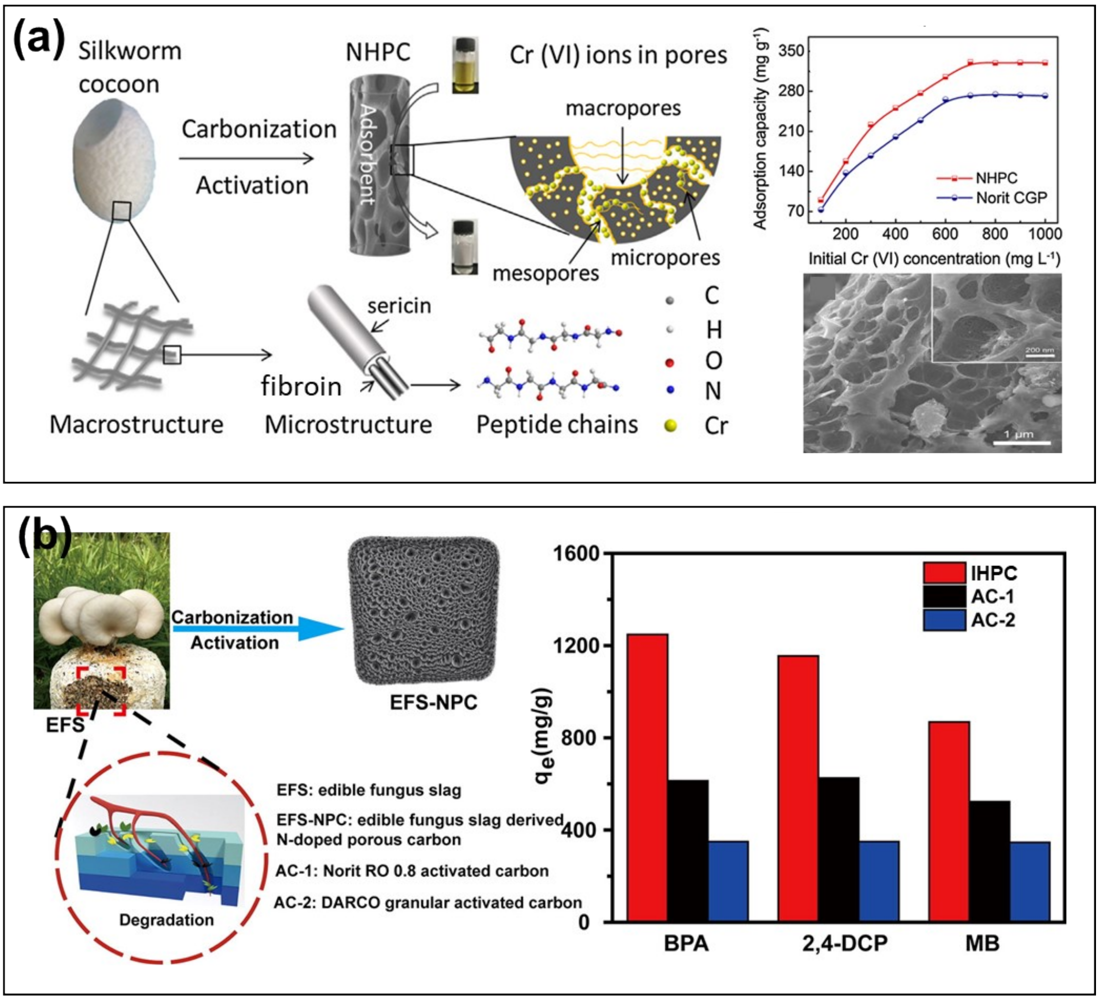

Fig. S4. (a) N,O-doped silkworm cocoon-based IHPC was fabricated to adsorb Cr(VI) (Sun et al., 2017), and (b) N-doped fungus slag-based IHPC was prepared to eliminate bisphenol A, 2,4-dichlorophenol and methylene blue (Cheng et al., 2019).

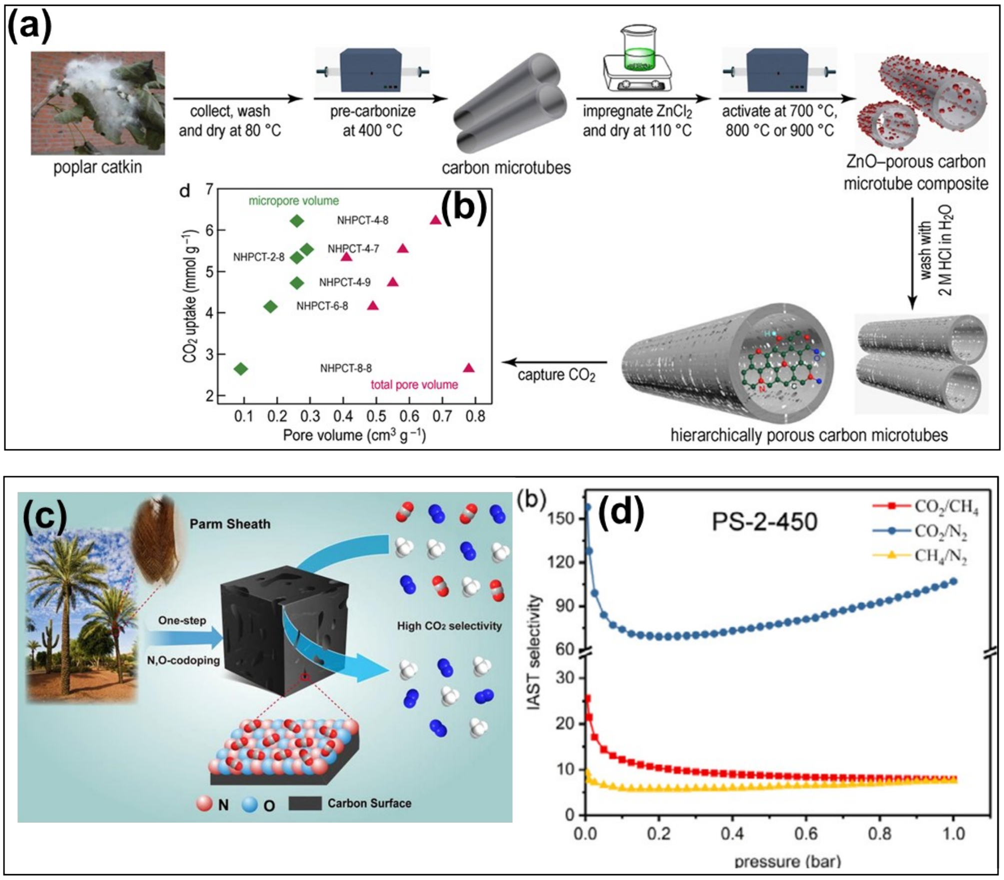

Fig. S5. (a, b) Poplar catkin-based IHPC was synthesized to capture CO_2 and the effects of the micropore ratio on the CO_2 uptake of poplar catkin-based IHPC (Chang et al., 2019); (c, d) palm sheath-based IHPC was fabricated to produce the high selectivity of CO_2 with CH_4 and H_2 (Liu et al., 2020).

References

Chang, B., Shi, W., Yin, H., Zhang, S., Yang, B. 2019. Poplar catkin-derived self-templated synthesis of N-doped hierarchical porous carbon microtubes for effective CO_2 capture. Chemical Engineering Journal, 358, 1507-1518.

Chen, L., Ji, T., Mu, L., Shi, Y., Wang, H., Zhu, J. 2017. Pore size dependent molecular adsorption of cationic dye in biomass derived hierarchically porous carbon. Journal of Environmental Management, 196, 168-177.

Chen, M.F., Yu, D., Zheng, X.Z., Dong, X.P. 2019. Biomass based N-doped hierarchical porous carbon nanosheets for all-solid-state supercapacitors. Journal of Energy Storage, 21, 105-112.

Cheng, J., Gu, J.-J., Tao, W., Wang, P., Liu, L., Wang, C.-Y., Li, Y.-K., Feng, X.-H., Qiu, G.-H., Cao, F.-F. 2019. Edible fungus slag derived nitrogen-doped hierarchical porous carbon as a high-performance adsorbent for rapid removal of organic pollutants from water. Bioresource Technology, 294, 122149.

Cuong, D.V., Liu, N.L., Nguyen, V.A., Hou, C.H. 2019. Meso/micropore-controlled hierarchical porous carbon derived from activated biochar as a high-performance adsorbent for copper removal. Science of The Total Environment, 692, 844-853.

Cuong, D.V., Matsagar, B.M., Lee, M., Hossain, M.S.A., Yamauchi, Y., Vithanage, M., Sarkar, B., Ok, Y.S., Wu, K.C.W., Hou, C.-H. 2021. A critical review on biochar-based engineered hierarchical porous carbon for capacitive charge storage. Renewable and Sustainable Energy Reviews, 145, 111029.

Dai, J.D., Qin, L., Zhang, R.L., Xie, A.T., Chang, Z.S., Tian, S.J., Li, C.X., Yan, Y.S. 2018. Sustainable bovine bone-derived hierarchically porous carbons with excellent adsorption of antibiotics: Equilibrium, kinetic and thermodynamic investigation. Powder Technology, 331, 162-170.

Du, Y., Chen, H., Xu, X., Wang, C., Zhou, F., Zeng, Z., Zhang, W., Li, L. 2020. Surface modification of biomass derived toluene adsorbent: hierarchically porous characterization and heteroatom doped effect. Microporous and Mesoporous Materials, 293, 109831.

Gao, F., Geng, C., Xiao, N., Qu, J.Y., Qiu, J.S. 2018. Hierarchical porous carbon sheets derived from biomass containing an activation agent and in-built template for lithium ion batteries. Carbon, 139, 1085-1092.

Hou, J., Cao, C., Idrees, F., Ma, X. 2015. Hierarchical porous nitrogen-doped carbon nanosheets derived from silk for ultrahigh-capacity battery anodes and supercapacitors. ACS Nano, 9(3), 2556-2564.

Huang, J., Chen, L., Dong, H., Zeng, Y., Hu, H., Zheng, M., Liu, Y., Xiao, Y., Liang, Y. 2017. Hierarchical porous carbon with network morphology derived from natural leaf for superior aqueous symmetrical supercapacitors. Electrochimica Acta, 258, 504-511.

Kim, J., Yi, Y., Peck, D.H., Yoon, S.H., Jung, D.H., Park, H.S. 2019. Controlling hierarchical porous structures of rice-husk-derived carbons for improved capacitive deionization performance. Environmental Science: Nano, 6(3), 916-924.

Liu, F., Zhang, Y., Zhang, P., Xu, M., Tan, T., Wang, J., Deng, Q., Zhang, L., Wan, Y., Deng, S. 2020. Facile preparation of N and O-rich porous carbon from palm sheath for highly selective separation of $CO_2/CH_4/N_2$ gas-mixture. Chemical Engineering Journal, 399, 125812.

Liu, J., Deng, Y., Li, X., Wang, L. 2016. Promising nitrogen-rich porous carbons derived from one-step calcium chloride activation of biomass-based waste for high performance supercapacitors. ACS Sustainable Chemistry & Engineering, 4(1), 177-187.

Liu, M., Xu, M., Xue, Y., Ni, W., Huo, S., Wu, L., Yang, Z., Yan, Y. 2018. Efficient capacitive deionization using natural basswood derived, free standing, hierarchically porous carbon electrodes. ACS Applied Materials & Interfaces.

Ouyang, H.B., Gong, Q.Q., Li, C.Y., Huang, J.F., Xu, Z.W. 2019. Porphyra derived hierarchical porous carbon with high graphitization for ultra-stable lithium-ion batteries. Materials Letters, 235, 111-115.

Qin, L., Zhou, Z.P., Dai, J.D., Ma, P., Zhao, H.B., He, J.S., Xie, A., Li, C.X., Yan, Y.S. 2016. Novel N-doped hierarchically porous carbons derived from sustainable shrimp shell for high-performance removal of sulfamethazine and chloramphenicol. Journal of the Taiwan Institute of Chemical Engineers, 62, 228-238.

Rybarczyk, M.K., Peng, H.J., Tang, C., Lieder, M., Zhang, Q., Titirici, M.M. 2016. Porous carbon derived from rice husks as sustainable bioresources: insights into the role of micro-/mesoporous hierarchy in hosting active species for lithium-sulphur batteries. Green Chemistry, 18(19), 5169-5179.

Shi, Q., Wang, Y., Zhang, X., Shen, B., Wang, F., Zhang, Y. 2020. Hierarchically porous biochar synthesized with $CaCO_3$ template for efficient Hg0 adsorption from flue gas. Fuel Processing Technology, 199, 106247.

Song, S.J., Ma, F.W., Wu, G., Ma, D., Geng, W.D., Wan, J.F. 2015. Facile self-templating large scale preparation of biomass-derived 3D hierarchical porous carbon for advanced supercapacitors. Journal of Materials Chemistry A, 3(35), 18154-18162.

Sun, J.T., Niu, J., Liu, M.Y., Ji, J., Dou, M.L., Wang, F. 2018. Biomass-derived nitrogen-doped porous carbons with tailored hierarchical porosity and high specific surface area for high energy and power density supercapacitors. Applied Surface Science, 427, 807-813.

Sun, J.T., Zhang, Z.P., Ji, J., Dou, M.L., Wang, F. 2017. Removal of Cr^{6+} from wastewater via adsorption with high-specific-surface-area nitrogen-doped hierarchical porous carbon derived from silkworm cocoon. Applied Surface Science, 405, 372-379.

Tian, Z.W., Qiu, Y., Zhou, J.C., Zhao, X.B., Cai, J.J. 2016. The direct carbonization of algae biomass to hierarchical porous carbons and CO_2 adsorption properties. Materials Letters, 180, 162-165.

Wang, Y., Gu, Y., Li, H., Ye, M., Qin, W., Zhang, H., Wang, G., Zhang, Y., Zhao, H. 2020. Electrodeposition of hierarchically amorphous FeOOH nanosheets on carbonized bamboo as an efficient filter membrane for As(III) removal. Chemical Engineering Journal, 392, 123773.

Wei, H.M., Chen, J., Fu, N., Chen, H.J., Lin, H.L., Han, S. 2018. Biomass-derived nitrogen-doped porous carbon with superior capacitive performance and high CO_2 capture capacity. Electrochimica Acta, 266, 161-169.

Wei, X., Zhang, Z.D., Qin, L., Dai, J.D. 2019. Template-free preparation of yeast-derived three-dimensional hierarchical porous carbon for highly efficient sulfamethazine adsorption from water. Journal of the Taiwan Institute of Chemical Engineers, 95, 532-540.

Xu, J.Q., Zhou, K., Chen, F., Chen, W., Wei, X.F., Liu, X.W., Liu, J.H. 2016. Natural integrated carbon architecture for rechargeable lithium-sulfur batteries. ACS Sustainable Chemistry & Engineering, 4(3), 666-670.

Yin, W.Q., Dai, D., Hou, J.H., Wang, S.S., Wu, X.G., Wang, X.Z. 2019. Hierarchical porous biochar-based functional materials derived from biowaste for Pb(II) removal. Applied Surface Science, 465, 297-302.

Yuan, C.J., Lin, H.B., Lu, H.Y., Xing, E.D., Zhang, Y.S., Xie, B.Y. 2016. Synthesis of hierarchically porous MnO2/rice husks derived carbon composite as high-performance electrode material for supercapacitors. Applied Energy, 178, 260-268.

Zhang, Y.C., You, Y., Xin, S., Yin, Y.X., Zhang, J., Wang, P., Zheng, X.S., Cao, F.F., Guo, Y.G. 2016. Rice husk-derived hierarchical silicon/nitrogen-doped carbon/carbon nanotube spheres as low-cost and high-capacity anodes for lithium-ion batteries. Nano Energy, 25, 120-127.

Zhao, Y., Ran, W., He, J., Song, Y., Zhang, C., Xiong, D.B., Gao, F., Wu, J., Xia, Y. 2015. Oxygen-rich hierarchical porous carbon derived from artemia cyst shells with superior electrochemical performance. ACS Applied Materials & Interfaces, 7(2), 1132-9.

Zhou, K., Ma, W., Zeng, Z., chen, R., Xu, X., Liu, B., Li, H., Li, H., Li, L. 2020. Waste biomass-derived oxygen and nitrogen co-doped porous carbon/MgO composites as superior acetone adsorbent: Experimental and DFT study on the adsorption behavior. Chemical Engineering Journal, 387, 124173.

Zhu, Y., Xu, G.Y., Zhang, X.L., Wang, S.J., Li, C., Wang, G.X. 2017. Hierarchical porous carbon derived from soybean hulls as a cathode matrix for lithium-sulfur batteries. Journal of Alloys and Compounds, 695, 2246-2252.